Inorganica Chimica Acta 434 (2015) 188–197

Contents lists available at ScienceDirect

Inorganica Chimica Acta

journal homepage: www.elsevier.com/locate/ica

Syntheses and structural studies on some new dithiophosphinato complexes of nickel(II), cobalt(II) and mixed pyridino complexes thereof

Ertuğrul Gazi Sağlam *

Department of Chemistry, Bozok University, 66900 Yozgat, Turkey

ARTICLE INFO

Article history:
Received 12 March 2015
Received in revised form 22 May 2015
Accepted 28 May 2015
Available online 9 June 2015

Keywords:
Thio-phosphorus complexes
Dithiophosphinic acid
Lawesson reagent
Pyridino complexes
X-ray structure
Raman spectroscopy

ABSTRACT

Four different, alkyl(4-methoxyphenyl)dithiophosphinic acid metal complexes, namely, trans-bis-[*iso*-propyl (4-methoxyphenyl)dithiophosphinato]nickel(II), **1**; bis-{[*iso*-propyl (4-methoxyphenyl)-dithiophosphinato]}cobalt(II), **2**; bis-{[*sec*-butyl (4-methoxyphenyl)-dithiophosphinato]}cobalt(II), **3** and bis-{[*iso*-amyl (4-methoxyphenyl)-dithiophosphinato]}cobalt(II), **4** were prepared. As **1** and **2** were synthesized for the first time, their structures were also elucidated. Starting with these four-coordinated complexes, novel, mixed (pyridino) dithiophosphinic acid complexes of Ni(II) and Co(II) were also prepared. These complexes were characterized by elemental analysis and NMR (^{1}H-, ^{13}C-, ^{31}P-); MS; FTIR; and Raman spectroscopies. TGA and DTA data were also made use of to support the structures revealed by spectroscopy. The magnetic susceptibilities of the complexes were measured to confirm the hybridization patterns and the geometries. The crystal structures of the cobalt pyridino-DTPA complexes were analyzed. X-ray analyses show that the P–S bonds in the complexes are essentially of the same order; that is, electron delocalization prevails.

© 2015 Elsevier B.V. All rights reserved.

1. Introduction

Until 1945, studies on dithiophosphinic acids (DTPAs) were scarce, probably due to their disagreeable odour; but as people discovered their technical importance, investigations have gradually intensified [1,2]. DTPAs and their derivatives find applications as additives of lubrication oils [3], aviation hydraulic [4] and pesticides [5]. Some Sn- and Sb-DTPA derivatives were discovered to be potentially effective in the chemotherapy of some tumours [6]. A commercially available DTPA derivative CYNAEX-301 (bis-(2,4,4-trimethylpentyl)dithiophosphinic acid) has found a considerable use in the extraction of lanthanides and actinides from nuclear wastes [7,8] and from waste water [9].

Various routes have been developed for the DTPA synthesis [10,11], the most general one being the addition reaction of Grignard reagents with perthiophosphonic acid anhydrides such as Lawesson reagent (LR). The DTPAs formed were further reacted with ammonia to form the easily crystallizable ammonium salts; facilitating a quick refinement of the DTPA. The ammonium salt is stable and can easily be converted to complexes when desired [12].

The DTPAs are strong chelate forming ligands for soft acid type metal cations. Their complexes generally display a four- or six-coordinated geometry [13–17]. Zinc and cadmium cations are known to form dimeric DTPA complexes [18]. The coordination geometries of these dimeric complexes are generally in chair conformation, but some zinc complexes are known to display boat conformation [19]. Some cobalt(II) and manganese(II) complexes of DTPAs are also known to display dimeric structures [20,21].

The metallic nuclei of some DTPA complexes may coordinate further ligands like ammonia and pyridine so as to increase their coordination numbers [22,23]. For example, a square-planar DTPA-Ni(II) complexes may coordinate one or two molecules of pyridine (or pyridine derivatives) to yield new, five- or six-coordinated complexes [24–26]. Aliphatic amines are also known to behave similarly to yield a six-coordinated structures [27]. Paramagnetic tetrahedral DTPA-Co(II) complexes have also been reported to coordinate one or two new Lewis bases to form five- or six-coordinated mixed complexes [28–30].

Single crystal X-ray studies on five- or six-coordinated DTPA-Ni(II) complexes are scarce, and even more so for DTPA-Co(II) species in the literature [31–34]. These types of mixed complexes are relatively unstable and especially the DTPA-Ni–Py compounds can easily give off the amine species if not kept at low temperatures [35].

* Tel.: +90 0354 242 10 21x2521; fax: +90 0354 242 10 22.
E-mail address: saglameg@gmail.com

http://dx.doi.org/10.1016/j.ica.2015.05.028
0020-1693/© 2015 Elsevier B.V. All rights reserved.

2. Experimental

2.1. Materials and Instruments

Analytical-grade LR, *iso*-propyl bromide, *sec*-butyl bromide and *iso*-amyl bromide were purchased from Merck and used directly without further purification. Benzene, chloroform, diethyl ether, methanol, ethanol, pyridine, $NiCl_2{\cdot}6H_2O$ and $CoCl_2{\cdot}6H_2O$ were purchased from Merck. Benzene and diethyl ether were distilled and dried before use.

The complexes, trans-bis-[*iso*-propyl (4-methoxyphenyl)dithiophosphinato]nickel(II), 1; bis-{[*iso*-propyl (4-methoxyphenyl)-dithiophosphinato]}cobalt(II), **2**; bis-{[*sec*-butyl (4-methoxyphenyl)-dithiophosphinato]}cobalt(II), **3** and bis-{[*iso*-amyl (4-methoxyphenyl)-dithiophosphinato]}cobalt(II), **4** were prepared as reported previously [36,37].

The LC/MS spectra were recorded with a Waters Micromass ZQ connected with Waters Alliance HPLC, using ESI(+) method, with the C-18 column. Magnetic susceptibilities were measured on a Sherwood Scientific magnetic susceptibility balance (Model MK1) at room temperature (25 °C). Melting points were measured with a Gallenkamp apparatus using a capillary tube. ^{1}H, ^{13}C{^{1}H} and ^{31}P{^{1}H} NMR spectra were recorded with a Varian Mercury (Agilent) 400 MHz FT spectrometer in $CDCl_3$. $SiMe_4$ (^{1}H, ^{13}C) and 85% H_3PO_4 (^{31}P) were used as standards. Chemical shifts (δ) are given in ppm. Thermogravimetric studies were performed on a Diamond TGA/DTA analyzer under a heating rate of 5 °C min^{-1}. The thermograms were recorded in the temperature range of 50–1000 °C. The measurements were carried out under a nitrogen flow of 200 mL min^{-1}. IR spectra were recorded on a Perkin Elmer Spectrum 400 FTIR spectrophotometer (200–4000 cm^{-1}) and are reported in cm^{-1} units. All Raman spectra were measured in the range of 4000–100 cm^{-1}, at room temperature, using a Renishaw in-Via Raman microscope, equipped with a Peltier-cooled CCD detectors (−70 °C). For Raman microscopy, a 50X objective was usually used and all the spectra were excited by the 785 line of a diode laser. Microanalyses were performed using a LECO CHNS-932 C elemental analyzer.

2.2. Syntheses of compounds

2.2.1. Preparation of ammonium iso-propyl (4-methoxyphenyl)dithiophosphinate], ***NH$_4$L***

NH_4L was prepared according to the literature [38]. NMR spectroscopic data and mass data are as follows: ^{1}H NMR (in D_2O): δ = 0.91 (dd, $^3J_{PH}$ = 20.4 Hz, $^3J_{HH}$ = 6.9 Hz, 6H, –CH–(C*H*$_3$)$_2$); 2.12 (m, H, –C*H*–); 3.73 (s, 3H, OC*H*$_3$); 6.92 (A-part of AA′MM′X, $^4J_{PH}$ = 2.2 Hz (J_{AX}), $N = J_{AM} + J_{AM'}$ = 8.9 Hz, 2H, *m*-H); 7.83 (M-part of AA′MM′X, $^3J_{PH}$ = 12.0 Hz (J_{MX}), N = 8.9 Hz, 2H, *o*-H). ^{13}C NMR (ppm, in D_2O): δ = 18.9 (s, –(*C*H$_3$)$_2$); 41.2 (d, J_{P-C} = 55.4 Hz, P–*C*H–); 58.3 (s, *C*H$_3$O–); 116.2 (d, $^3J_{P-C}$ = 12.90 Hz, Ar–C$_{meta}$); 133.5 (d, J_{P-C} = 78.6 Hz, P–C$_{arom}$); 135.4 (d, $^2J_{P-C}$ = 11.6 Hz, Ar–C$_{ortho}$); 163.5 (s, CH$_3$O–*C*). ^{31}P NMR (in D_2O): δ = 76.1. LC/MS MS: *m*/*z* 247.2 ([M+H]$^+$, 100%), 205.0 ([M−(*iso*-C$_3$H$_7$)]$^+$, 41%).

2.2.2. Preparation of complexes

2.2.2.1. Trans-bis-[iso-propyl (4-methoxyphenyl)dithiophosphinato] nickel(II), ***1***. A solution of $NiCl_2{\cdot}6H_2O$, (0.29 g, 1.24 mmol) in methanol (10 mL) was added to the methanolic solution (25 mL) of NH_4L (0.65 g, 2.47 mmol). The mixture was heated gently. The resulting solution was left to stand overnight and needle-like crystals formed. The deep blue color crystalline solid was filtered off and recrystallized from methanol or chloroform. Yield: 0.47 g (70%). M.P. 152 °C. Diamagnetic. ^{1}H NMR (in $CDCl_3$): δ = 1.20 (dd, $^3J_{PH}$ = 21.0 Hz, $^3J_{HH}$ = 7.0 Hz, 6H, –CH–(C*H*$_3$)$_2$), 2.21 (m, H, –C*H*–), 3.85 (s, 3H, OC*H*$_3$), 6.96 (A-part of AA′MM′X, $^4J_{PH}$ = 2.2 Hz (J_{AX}), N = 9.0 Hz, 2H, *m*-H), 7.56 (M-part of AA′MM′X, $^3J_{PH}$ = 12.5 Hz (J_{MX}), N = 9.0 Hz, 2H, *o*-H). ^{13}C NMR (ppm, $CDCl_3$): δ = 15.1 (s, –(CH$_3$)$_2$), 38.5 (d, J_{P-C} = 42.6 Hz, P–*C*H–), 55.7 (s, *C*H$_3$O–), 114.0 (d, $^3J_{P-C}$ = 14.6 Hz, Ar–C$_{meta}$), 126.1 (d, J_{P-C} = 66.7 Hz, P–C$_{arom}$) 131.4 (d, $^2J_{P-C}$ = 13.1 Hz, Ar–C$_{ortho}$), 162.6 (s, CH$_3$O–*C*). ^{31}P NMR (in $CDCl_3$): δ = 96.6. LC/MS MS: *m*/*z* 548.9 ([M]$^+$, 9%); 334.9 ([M−((*iso*-C$_3$H$_7$)(CH$_3$OC$_4$H$_9$)PS)]$^+$, 100.0%); 302.9 ([M−((*iso*-C$_3$H$_7$)(CH$_3$OC$_4$H$_9$)PS$_2$)]$^+$, 88.3%). *Anal.* Calc. for $C_{20}H_{28}NiO_2P_2S_4$ (549.33 g mol^{-1}): C, 43.73; H, 5.14; S, 23.35. Found: C, 43.46; H, 4.93; S, 23.60%.

2.2.2.2. Bis-{bis[iso-propyl (4-methoxyphenyl)dithiophosphinato] cobalt(II)}, ***2***. A solution of $CoCl_2{\cdot}6H_2O$ (0.29 g, 1.24 mmol) in methanol (10 mL) was added to the methanolic solution (25 mL) of NH_4L (0.65 g, 2.47 mmol. The mixture was heated gently. The resulting solution was left to stand overnight to obtain crystals. The green crystalline solid was filtered off and recrystallized from ethanol. Yield: 0.42 g (63%). M.P. 180–182 °C. μ_{eff} = 4.10 B.M. LC/MS MS: *m*/*z* 1121.6 ([M+Na]$^+$, 7.4%); 852.6 ([M−((*iso*-C$_3$H$_7$)(CH$_3$OC$_4$H$_9$)PS$_2$)]$^+$, 100.0%); 549.4 ([1/2M]$^+$, 23,2%). *Anal.* Calc. for $C_{40}H_{56}Co_2O_4P_4S_8$ (1099.15 g mol^{-1}): C, 43.71; H, 5.14; S, 23.34. Found: C, 43.48; H, 4.89; S, 23.32%.

2.2.2.3. Preparation of pyridino complexes.

2.2.2.3.1. Pyridino-bis[iso-propyl (4-methoxyphenyl)-dithiophosphinato] cobalt(II), ***5***. To a sample of **2**, (0.5 g, 0.5 mmol) dissolved in ethanol (30 mL), 0.04 g (0.4 mmol) of pyridine was added dropwise with constant stirring. Left aside for a few days, a mat greenish/blue solid formed. This solid was filtered and recrystallized from methanol. Yield: 0.19 g (66%). M.P., decomposition upon heating. μ_{eff} = 4.51 B.M. LC/MS MS: *m*/*z* 628.9 ([M]$^+$, 100.0%); 382.9 ([M−(Py+((*iso*-C$_3$H$_7$)(CH$_3$OC$_4$H$_9$)PS$_2$)]$^+$, 16.9%); 852.8 ([Co$_2$(*iso*-C$_3$H$_7$)(CH$_3$OC$_4$H$_9$)PS$_2$)$_3$]$^+$, 52.3%); 549.4 ([M−2Py]$^+$, 28,3%). *Anal.* Calc. for $C_{25}H_{33}NCoO_2P_2S_4$ (628.68 g mol^{-1}): C, 47.76; H, 5.29; N, 2.23; S, 20.40. Found: C, 47.52; H, 5.11; N, 2.22; S, 20.53%.

2.2.2.4. Preparation of dipyridino complexes.

2.2.2.4.1. Bis-pyridino-bis[iso-propyl (4-methoxyphenyl)dithiophosphinato]}nickel(II), ***6***. To a sample of **1** (0.5 g, 1.0 mmol) dissolved in chloroform (30 mL) an excess (5–6 mL) of ethanolic pyridine solution (1:1, v/v) was added dropwise with constant stirring. Left aside for two days, a green solid formed. This solid was filtered and recrystallized from ethanol. Yield: 0.61 g (95%). M.P., decomposition upon heating. μ_{eff} = 2.95 B.M. LC/MS MS: *m*/*z* 729.8 ([M+Na]$^+$, 14.4%); 627.9 ([M−Py]$^+$, 68.7%); 381.9 ([(Py)$_2$M−((*iso*-C$_3$H$_7$)(CH$_3$OC$_4$H$_9$)PS$_2$)]$^+$, 100.0%); 302.9 ([M−(2Py+(*iso*-C$_3$H$_7$)(CH$_3$OC$_4$H$_9$)PS$_2$)]$^+$, 18.2%). *Anal.* Calc. for $C_{30}H_{38}N_2NiO_2P_2S_4$ (707.54 g mol^{-1}): C, 50.93; H, 5.41; N, 3.96; S, 18.13. Found: C, 50.81; H, 5.36; N, 3.95; S, 18.43%.

2.2.2.4.2. Bis-pyridino-bis[iso-propyl (4-methoxyphenyl)dithiophosphinato]cobalt(II), ***7***. To a sample of **2**, (0.55 g, 0.5 mmol) dissolved in $CHCl_3$ (30 mL) an excess (5–6 mL) of ethanolic pyridine solution (1:1, v/v) was added dropwise with constant stirring. Left aside for two days, a mat blue solid formed. This solid was filtered and recrystallized from ethanol. Yield: 0.56 g (88%). M.P., decomposition upon heating. μ_{eff} = 5.16 B.M. LC/MS MS: *m*/*z* 731.9 ([M+Na]$^+$, 2.9%); 628.9 ([M−Py]$^+$, 100.0%); 852.8 ([Co$_2$((*iso*-C$_3$H$_7$)(CH$_3$OC$_4$H$_9$)PS$_2$)$_3$]$^+$, 40.9%); 549,9 ([M−2Py]$^+$, 40.9%). *Anal.* Calc. for $C_{30}H_{38}N_2CoO_2P_2S_4$ (707.77 g mol^{-1}): C, 50.91; H, 5.41; N, 3.96; S, 18.12. Found: C, 50.69; H, 5.37; N, 4.04; S, 18.21%.

2.2.2.4.3. Bis-pyridino-bis[sec-butyl (4-methoxyphenyl)dithiophosphinato]cobalt(II), ***8***. To a 0.44 g (0.4 mmol) sample of **3**, dissolved in $CHCl_3$ (30 mL) an excess (5–6 mL) of ethanolic pyridine solution (1:1, v/v) was added dropwise with constant stirring. Left aside

for two days, a mat blue solid formed. This solid was filtered and recrystallized from ethanol. Yield: 0.49 g (80%). M.P., decomposition upon heating. μ_{eff} = 4.98 B.M. LC/MS MS: *m/z* 759.8 ($[M+Na]^+$, 4.2%); 656.9 ($[M-Py]^+$, 40.0%); 475.9 ($[M-((sec\text{-}C_4H_9)(CH_3OC_4H_9)PS_2)]^+$, 100.0%); 396.8 ($[M-(Py+(sec\text{-}C_4H_9)(CH_3OC_4H_9)PS_2)]^+$, 35.9%). *Anal.* Calc. for $C_{32}H_{42}N_2CoO_2P_2S_4$ (735.83 g mol^{-1}): C, 52.23; H, 5.75; N, 3.81; S, 17.43. Found: C, 52.30; H, 5.63; N, 3.80; S, 17.53%.

2.2.2.4.4. Bis-pyridino-bis[iso-amyl(4-methoxyphenyl)-dithiophosphinato]cobalt(II), ***9***. To a 0.55 g (0.5 mmol) sample of **4**, dissolved in $CHCl_3$ (30 mL) an excess (5–6 mL) of ethanolic pyridine solution (1:1, v/v) was added dropwise with constant stirring. Left aside for two days, a mat blue solid formed. This solid was filtered and recrystallized from ethanol. Yield: 0.57 g (90%). M.P., decomposition upon heating. μ_{eff} = 5.02 B.M. (LC/MS MS: *m/z* 787.8 ($[M+Na]^+$, 7.3%); 685.0 ($[M-Py]^+$, 98.0%); 606.0 ($[M-2Py]^+$, 12.9%); 489,9 ($[M-((iso\text{-}amyl)(CH_3OC_4H_9)PS_2)]^+$, 100.0%); 410.8 ($[M-(Py+(iso\text{-}amyl)(CH_3OC_4H_9)PS_2)]^+$, 56.9%); 261.8 ($[(M-(2Py+(iso\text{-}amyl)_2(CH_3OC_4H_9)PS_2)]^+$, 96.1%). *Anal.* Calc. for $C_{34}H_{46}CoN_2O_2P_2S_4$ (763.88 g mol^{-1}): C, 53.46; H, 6.07; N, 3.67; S, 16.79. Found: C, 52.35; H, 6.16; N, 3.59; S, 16.83%.

2.3. X-ray crystallography

Single-crystal X-ray diffraction analyses of **5**, **7**, **8** and **9** were performed on a Bruker Kappa APEXII CCD area-detector diffractometer using Mo Kα radiation (λ = 0.71073 Å) at a temperature of 100 K. Structures were solved by direct methods [39] and refined by full-matrix least squares against F^2 using all data [39]. All non-H atoms were refined anisotropically. H atoms were positioned geometrically at distances of 0.93 Å (aromatic CH), 0.98 Å (CH), 0.97 Å (CH_2) and 0.96 Å (CH_3) from the parent C atoms; a riding model was used during the refinement process and the U_{iso}(H) values were constrained to be xU_{eq} (carrier atom), where x = 1.2 for CH and CH_2, and x = 1.5 for CH_3. Experimental data are listed in Table 1.

3. Result and discussion

Four different, four-coordinated alkyl *p*-methoxyphenyl dithiophosphinic acid metal complexes of the structures below were prepared.

The details of the synthesis procedure were given elsewhere [36–38]. Of these four compounds, **1** and **2** were synthesized for the first time; so these compounds were also characterized spectroscopically. The characterizations of the other two structures have already been published [36,37].

Starting with the four-coordinated complexes, novel, mixed (pyridino) DTPA complexes of Ni(II) and Co(II) cations were prepared. The synthesis procedure and the structures of the five complexes are summarized in Scheme 1.

3.1. Spectroscopic studies

3.1.1. IR and Raman spectra

The asymmetric and symmetric (PS) stretching signals (ν_{asym} and ν_{sym}) of the complexes appear in the regions of 653–617 cm^{-1} and 542–517 cm^{-1}, respectively. In the Raman spectra, similar signals appear in the regions of 664–605 cm^{-1} and 549–524 cm^{-1}, respectively.

The metal-sulfur stretching vibration signals give rise to the signals between 200 and 400 cm^{-1} (257–340 cm^{-1} for IR; 255–339 cm^{-1} for Raman). Mixed pyridine complexes display metal-nitrogen stretching signals (229–273 cm^{-1} for IR and 229–274 cm^{-1} for Raman), as well as metal-sulfur vibrations.

In the IR spectra, the characteristic ν_{N-H} band is observed at 3183 cm^{-1} for NH_4L; this band is absent in the spectra of the complexes **1** and **2**, confirming the exclusion of the NH_4^+ ion.

The frequencies of the corresponding signals in the IR and the Raman spectra of the same compound are quite comparable as expected. All these values are in agreement with the literature [18,42–45]. The prominent peaks are given in Table 2.

3.1.2. NMR spectra

The DTPA complexes of **2**, **5**, **6**, **7**, **8** and **9** are all paramagnetic. Their ambient temperature NMR spectra were not sought for.

The ^{1}H NMR data of the compound NH_4L and **1** are given in the section Experimental. The methyl protons of the *iso*-propyl group do not display any diasterotopic effect and appear simply as a doublet of doublets due to couplings to phosphorus and the –C*H* proton. Aromatic protons and the phosphorus nucleus together constitute a typical AA′MM′X spin system; but the couplings between the protons that are *meta*- and *para*- to each other are so close to zero that the signals effectively reduces to that of an AMX system. The ^{1}H NMR spectrum of the ligand (NH_4L) displays the same features.

^{13}C NMR data relating to ligand and the complex are given in the section Experimental. Here again, no diasterotopic differentiation between the –CH_3 carbon of the *iso*-propyl group is discernable. The two-bond ^{31}P–^{13}C coupling for the aromatic carbon atoms *ortho*- to the phosphorus are observed to be 12.9 Hz for the ligand and 14.6 Hz for the complex. The single bond ^{31}P–^{13}C coupling of the *ipso* carbon appears to have been reduced from 78.6 Hz (in the ligand) to 66.7 Hz (in the complex). In tetrahedral complexes, this coupling remains almost the same with that of the ligand [unpublished results found for the Zinc(II) and Cadmium(II)]. This is presumably due to the narrower "S–Ni–S" angles in the square planar geometry. A less striking tendency is observable in the one-bond J_{PC} for the central carbon of the *iso*-propyl group (roughly, 13 Hz reduction in the Ni-complex compared to 4–6 Hz for the tetrahedral complexes). To our surprise, the methyl carbons of the *iso*-propyl- group display no coupling to the phosphorus at all; both in the ligand and the complex. Near zero two bond ^{31}P–^{13}C couplings are not rare anyway [46,47], (and also unpublished results for the Zinc(II) and Cadmium(II) complexes of the same ligand).

^{31}P NMR spectra of NH_4L and **1** show singlets at 76.08 and 95.6 ppm, respectively. The large complex induced shift in the δ values reflects both the strength of the coordination bond and also the bond angle strain due to formation of planar geometry.

3.1.3. Mass spectra

The mass spectra of the complexes **1**, and **5** display molecular ion peaks. The other five complexes display no molecular ions, but $[M+Na]^+$ peaks. The sodium ions come from the buffer solution used in the ionization process in the LC/ES system. The natural abundance of isotopes are observable in the structure of the molecular ion signals. Reminiscent signal structures are reported for similar compounds [48].

Monomeric complex **1** displays an ion corresponding to the molecular ion minus of $((iso\text{-}C_3H_7)(CH_3OC_4H_9)PS_2)$ group. In the spectra of the dimeric complexes, mass peaks attributable to the ions formed by the removal of one and two $((iso\text{-}C_3H_7)(CH_3OC_4H_9)PS_2)$ groups are clearly observable.

Pyridino-Metal complexes, except for **5** display ions formed by the removal of one Py group. Other peaks are the same with those observed for **2** as expected.

The patterns of disintegration are compatible with those reported for similar structures [49–52] (see Fig. 1).

Table 1
X-ray experimental data for **5**, **7**, **8** and **9**.

Complex	**5**	**7**	**8**	**9**
Empirical Formula	$C_{25}H_{33}CoNO_2P_2S_4$	$C_{30}H_{38}CoN_2O_2P_2S_4$	$C_{32}H_{42}CoN_2O_2P_2S_4$	$C_{34}H_{46}CoN_2O_2P_2S_4$
Color/shape	green/block	purple/block	purple/block	purple/block
Formula weight	628.63	707.73	735.84	763.84
Temperature (K)	100(2)	100(2)	100(2)	100(2)
Radiation, graphite monochr.	Mo Kα (λ = 0.71073)			
Crystal system	triclinic	triclinic	monoclinic	monoclinic
Space group	$P\bar{1}$	$P\bar{1}$	$P2_1/n$	$P2_1/n$
a (Å)	9.8638(3)	9.4217(2)	10.9577(1)	12.4584(5)
b (Å)	11.1899(3)	10.1651(3)	9.6573(2)	9.5076(4)
c (Å)	15.1563(4)	10.4312(3)	17.1587(1)	16.0729(7)
α (°)	92.319(1)	77.305(3)	90	90
β (°)	107.820(1)	70.780(2)	103.361(1)	101.708(2)
γ (°)	110.123(1)	62.629(2)	90	90
Volume (Å^3)	1475.38(7)	834.94(4)	1766.62(4)	1864.22(14)
Z	2	1	2	2
Absorption coefficients (mm^{-1})	0.996	0.89	0.844	0.803
D_{calc} (mg m^{-3})	1.415	1.408	1.383	1.361
Maximum crystal dimension (mm)	0.13X0.23X0.35	0.20X0.25X0.36	0.20X0.23X0.34	0.22X0.28X0.34
θ_{max} (°)	28.44	28.40	25.85	28.30
Reflections measured	7382	4182	3401	4584
Range of h, k, l	$-13 < h < 13$, $-14 < k < 14$, $-18 < l < 20$	$-12 < h < 12$, $-13 < k < 13$, $-13 < l < 13$	$-13 < h < 13$, $-11 < k < 11$, $-20 < l < 20$	$-16 < h < 16$, $-12 < k < 10$, $-11 < l < 21$
Diffractometer/scan	Bruker Kappa APEX II / phi and w			
No of reflections with $I > 2\sigma(I)$	6606	3499	3258	3990
Corrections applied	Lorentz polarization			
Computer programs	SHELXS-97 [39], SHELXL-97 [39], ORTEP-3[40]			
Source of scatter. Factors	International Table for X-ray Crystallography [41]			
Structure solution	direct methods			
Treatment of hydrogen atoms	geometric calculation			
No. of parameters varied	316	190	199	205
Goodness-of-fit (GOF)	1.106	1.030	1.193	1.079
$R = \|\|F_o\| - \|F_c\|\|/\|F_o\|$	0.0243	0.0320	0.0571	0.0283
R_w	0.0756	0.0840	0.1546	0.0776
$(\Delta\rho)_{max}$ (e Å^{-3})	0.475	0.460	2.544	0.545
$(\Delta\rho)_{min}$ (e Å^{-3})	−0.354	−0.270	−1.196	−0.520

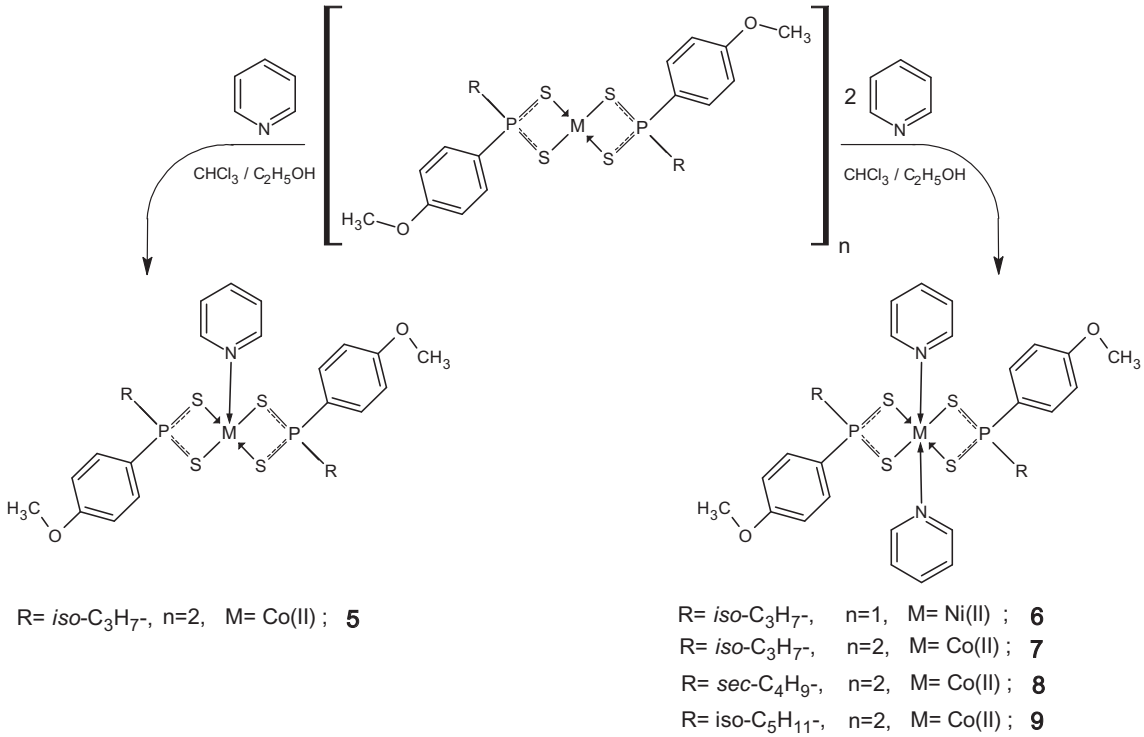

Scheme 1. Synthesis reaction of DTPA pyridino complexes.

Table 2
Selected FTIR and Raman (R) data (cm^{-1}) assignment of significant bands.

Compound	$\nu_{(asym)}$ (PS)		$\nu_{(sym)}$ (PS)		$\nu_{(M-S)}$		$\nu_{(M-N)}$		$\nu_{(N-H)}$	
	IR	R	IR	R	IR	R	IR	R	IR	R
NH_4L	544;534	535	491	488	–	–	–	–	3183	–
1	641;615	639;613	555	557	257	255	–	–	–	–
2	655;637	650;633	552;526	552;526	286	284	–	–	–	–
5	661;640	654;630	551;528	551;529	340	339	236	234	–	–
6	649;621	651;612	531	558;532	293	296	256	256	–	–
7	648;619	650;629	553;526	556;531	324	321	252	252	–	–
8	644;632	648;633	544;527	541;525	331	328	273	274	–	–
9	654;638	653;627	541;526	549;528	330	330	229	229	–	–

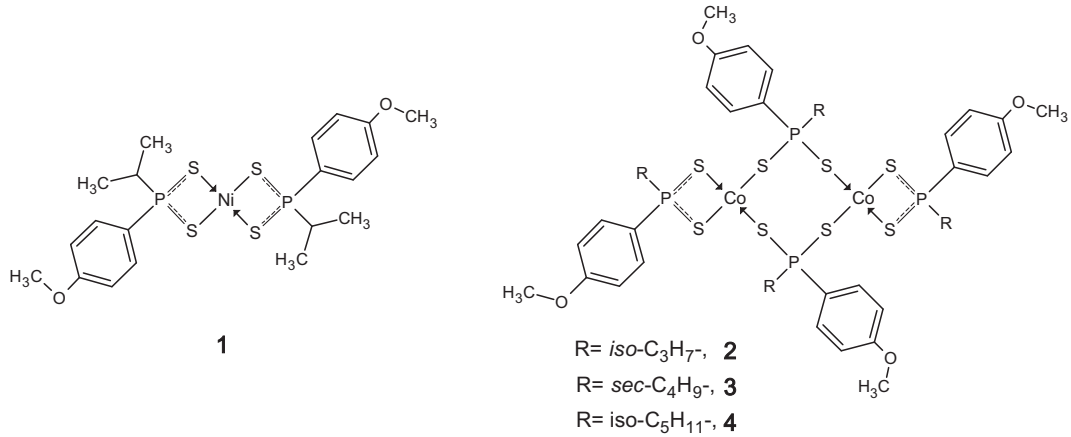

Fig. 1. Structure of nickel(II) and cobalt(II) DTPA complexes.

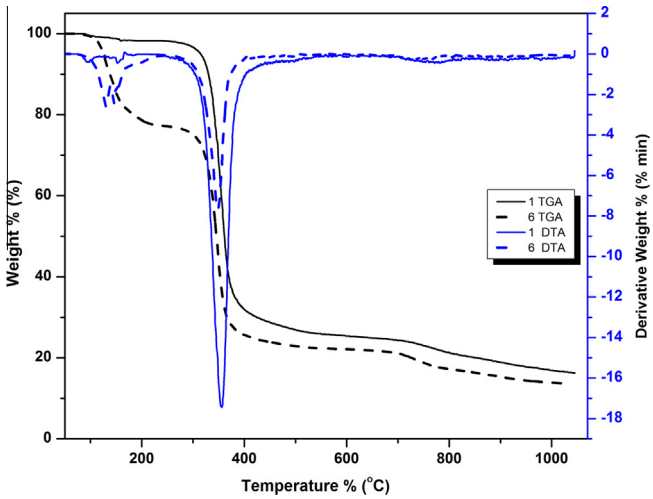

Fig. 2. TGA/DTA curves of **1** and **6**.

3.2. Thermal gravimetric studies (TGA/DTA)

TGA/DTA curves of the complexes are given in Figs. 2–4. A close investigation of the curves indicate that all the complexes thermally decompose in the interval of 300–380 °C. The stoichiometric mass percentage of the residue at 380–700 °C tentatively suggest that metal thiophosphites are formed.

The TGA curve of **1** shows a sudden mass decrease between 355 and 380 °C leaving back a residue of which mass (~35%) corresponds to the salts $NiPS_3$ roughly. Powder XRD spectrum of the thermal decomposition product of **1** at 400 °C under argon atmosphere (Fig. SM1 (supplementary material)) confirms that the product is indeed nickel(III)thiophosphite. A further decomposition between 380 and 800 °C leaves back a final residue of a mass (~16.5%) corresponding to NiS.

The thermal decomposition of **6** starts with the loss of two pyridine molecules in the interval 90–170 °C. The decomposition is endothermic as expected. Successive removal of pyridine moieties are discernable. The loss of other organic groups occurs between 170 and 380 °C. What remains back is, most probably, $NiPS_3$ as the mass (~26%) suggests. Powder XRD spectrum of thermal decomposition product at 400 °C supports the above conclusion (Fig. SM2). This salt gradually decomposes after 680 °C and at temperatures above 1000 °C, the final residue appears to be NiS.

The TGA curve of **2** displays a sudden mass decrease between 280 and 490 °C which indicates the loss of organic moieties. At 490 °C, the residue is probably $CoPS_3$ (plus some carbon) as the mass percentage (~40%) indicates. Powder XRD spectrum of the residue supports this assertion (Fig. SM3). This product decompose gradually up to 1000 °C and the decomposition appears continuing even at that temperature.

The TGA curve of **5** resembles to that of **1** and reflects the fact that the final residue at 710 °C is CoS.

The complex **7** starts decomposing at 110 °C and displays a weight loss of 22.5% at 250 °C which corresponds to the loss of two pyridine molecules. The major loss of other organic moieties occur between 250 and 380 °C leaving back a residue of which mass corresponds to some 30% of the original sample. This residue is most probably $CoPS_3$. A gradual decomposition is observed up to 950 °C leaving behind a final residue with a 13% mass which corresponds to CoS.

The thermal decomposition of **8** starts at 100 °C and at 200 °C, a weight loss 21% is observed reflecting the leave of two pyridine molecules. Loss of other organic moieties is observed between 300 and 400 °C and the mass of the residue (~29% of the original) corresponds approximately to $CoPS_3$ plus some carbon. This residue decomposes gradually leaving CoS behind.

The TGA graph relating to the complex **9** shows a decomposition between 80 and 260 °C. Obviously, this decomposition matches with the loss of two pyridine molecules which corresponds to a 21.6% mass loss. The remaining mass further decomposes between 260 and 510 °C. The residue corresponds to the 22% of the original and probably comprises $CoPS_3$ and some CoS. This residue further decompose between 510 and 1000 °C to leave CoS as the final mass.

3.3. Descriptions of the crystal structures

The X-ray structural determinations of **5**, **7**, **8** and **9** confirm the assignments of their structures from spectroscopic data. Selected bond lengths and angles are given in Table 3. The molecular structures along with the atom-numbering schemes are depicted in Figs. 5–8.

In complexes **7**, **8** and **9**, the Co atoms are located on inversion centers and coordinated by four symmetry-related S atoms. P–S bond lengths are not indicative of different bond orders. Despite the asymmetrical nature of the structures, the difference between the bond lengths hardly exceeds 0.03 Å which leads to the

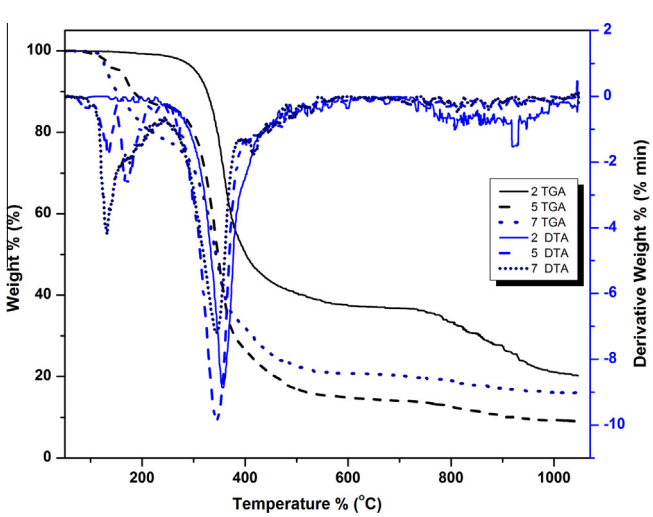

Fig. 3. TGA/DTA curves of **2**, **5** and **7**.

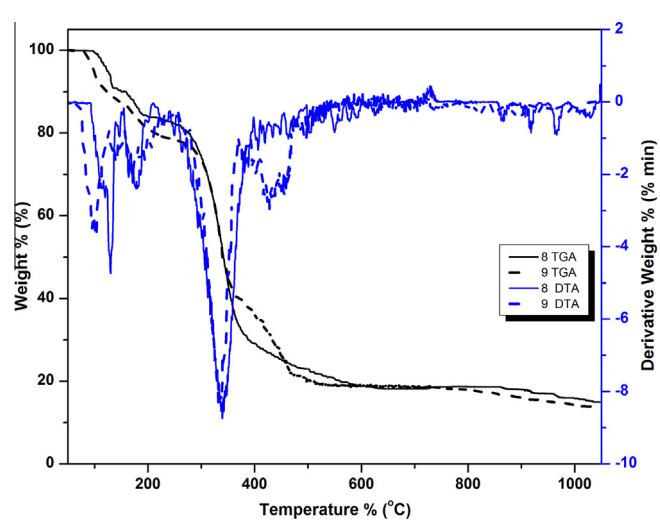

Fig. 4. TGA/DTA curves of **8** and **9**.

Table 3
Selected bond lengths (Å) and angles (°) for **5**, **7**, **8** and **9**.

Complex	**5**	**7**	**8**	**9**
Co1–N1	2.0665(15)	2.1731(15)	2.169(3)	2.1825(14)
Co1–S1	2.3330(5)	2.5721(4)	2.5510(10)	2.5114(4)
Co1–S2	2.6019(5)	2.5212(4)	2.5363(9)	2.5418(4)
Co1–S3	2.3385(4)			
Co1–S4	2.5536(5)			
P1–S1	2.0277(6)	2.0086(6)	2.0092(13)	2.0125(6)
P1–S2	1.9929(6)	2.0106(6)	2.0108(13)	2.0098(6)
P2–S3	2.0253(5)			
P2–S4	1.9983(5)			
P1–C1	1.8035(16)	1.8146(17)	1.813(4)	1.8077(17)
P1–C8	1.8331(17)	1.8355(18)	1.839(4)	1.8152(16)
P2–C11	1.8041(16)			
P2–C18	1.8305(17)			
S1–Co1–N1	122.02(4)	90.04(4)	90.73(9)	90.78(4)
S2–Co1–N1	90.64(4)	90.07(4)	89.81(8)	90.32(4)
S3–Co1–N1	111.90(4)			
S4–Co1–N1	95.45(4)			
S1–Co1–N1^{i}		89.96(4)	89.27(9)	89.22(4)
S2–Co1–N1^{i}		89.93(4)	90.19(8)	89.68(4)
S1–Co1–S2	82.833(15)	80.678(13)	81.03(3)	98.185(13)
S1–Co1–S2^{i}		99.322(13)	98.97(3)	81.815(13)
S1–Co1–S3	126.043(18)			
S1–Co1–S4	92.880(15)			
S2–Co1–S4	173.793(16)			
S2–Co1–S3	95.077(15)			
S3–Co1–S4	83.791(14)			
S1–P1–S2	108.88(2)	110.24(6)	110.59(6)	110.71(3)
S1–P1–C1	109.93(5)	110.25(6)	109.32(13)	109.20(5)
S1–P1–C8	109.23(6)	110.44(6)	109.71(15)	109.47(6)
S2–P1–C1	112.61(6)	110.22(6)	110.82(13)	111.18(6)
S2–P1–C8	111.27(6)	110.29(6)	111.09(15)	110.37(6)
C1–P1–C8	104.84(7)	105.30(8)	105.16(18)	105.78(8)
S3–P2–S4	108.76(2)			
S3–P2–C11	111.06(6)			
S3–P2–C18	109.11(6)			
S4–P2–C18	111.38(6)			
C11–P2–C18	105.64(7)			
P1–S1–Co1	87.099(19)	83.869(18)	82.05(4)	83.114(18)
P1–S2–Co1	80.755(18)	85.177(18)	82.40(4)	82.381(18)
P2–S3–Co1	86.111(18)			
P2–S4–Co1	81.059(17)			

Symmetry codes: (i) $-x+2, 1-y, 1-z$ (for **7**), $-x, -y, -z$ (for **8**) and $-x, -y, -z$ (for **9**).

conclusion that electron delocalization prevails in the PS_2^- groups. On the other hand, in the compound **5**, the Co–S bond-lengths differ considerably (2.3330 Å for Co1–S1 and 2.6019 Å for Co1–S2). This is attributed to the packing effects aggravated by the extremely asymmetrical structure of the compound. In the structures studied, the average Co–S bond lengths and S-Co-S bond angles for the complex **5, 7, 8** and **9** are 2.4568(5) Å and 88.645(15)°; 2.5466(4) Å and 90.000(13)°; 2.5437(10) Å and 90.00(3)°; and 2.5266(4) Å and 90.000(13)° respectively. That these angles are equal/very close to 90° is a clear indication of planar structures for the P–S–M–S moieties. For the same compounds, the average P–S bond lengths and S–P–S bond angles are 2.0111(6) Å and 108.82(2)°; 2.0096(6) Å and 110.24(6)°; 2.0100(13) Å and 110.59(6)°; 2.0112(6) Å and 110.71(3)°. On the other hand, the average P–S–Co bond angles are 83.756(18)°, 84.523(18)°, 82.23(4)° and 82.748(18)° for **5, 7, 8** and **9**, respectively (Table 3). The Co–S and P–S bond lengths, and S–Co–S and S–P–S bond angles are in good agreement with the corresponding average values [2.477(1) Å and 2.075(2) Å, and 87.29(5)° and 108.68(8)°, respectively] in [Co(4-NH_2-Py)(*iso*-C_4H_9)$_2$$PS_2$)$_2$] [34].

In compound **5**, in the four-membered rings A (Co1/S1/S2/P1) and B (Co1/S3/S4/P2), the angles between the (Co1/S1/S2) and (S1/S2/P1) and between the (Co1/S3/S4) and (S3/S4/P1) planes are 172.45(2)° and 173.90(2)°, indicating 7.55(2)° and 6.10(2)° bucklings with total wrinkles of 0.1757(9) Å and 0.1523(9) Å, respectively [53]. Thus, A and B rings may be called to have twisted-chair conformations. Similarly, in compounds **8** and **9**, in the four-membered rings A (Co1/S1/S2/P1), the angles between the (Co1/S1/S2) and (S1/S2/P1) planes are 157.11(4)° and 168.98(2)°, indicating 22.89(4)° and 11.02(2)° bucklings with total wrinkles of 0.4002(10) Å and −0.0462(1) Å, respectively [53]. So, A rings conveniently be called to have twisted-chair conformations. But, in compound **7**, the four-membered ring A (Co1/S1/S2/P1) is planar with a maximum deviation of 0.0197(5) Å for atom P1, and it is oriented with respect to the phenyl (C1–C6) and pyridine (N1/C11-C15) rings at dihedral angles of 69.33(4)° and 88.72(4)°, respectively.

In compound **5**, the Co1 atom has a distorted trigonal bipyramidal coordination (T = 0.8) with the N1 atom at one apex. The

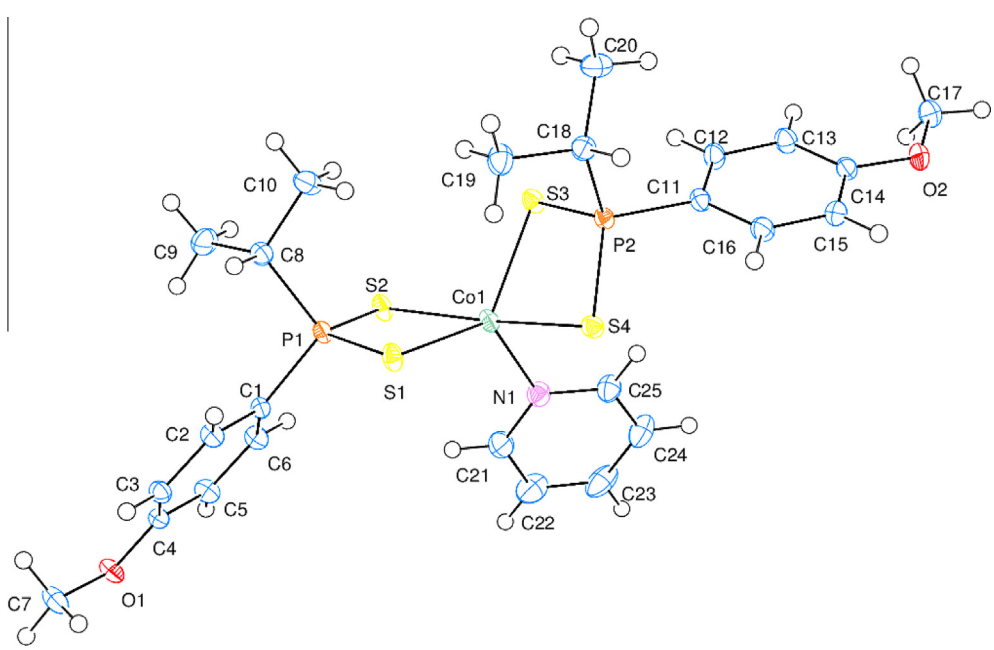

Fig. 5. An ORTEP-3 [40] view of **5** with the atom-numbering scheme. The thermal ellipsoids are drawn at the 50% probability level.

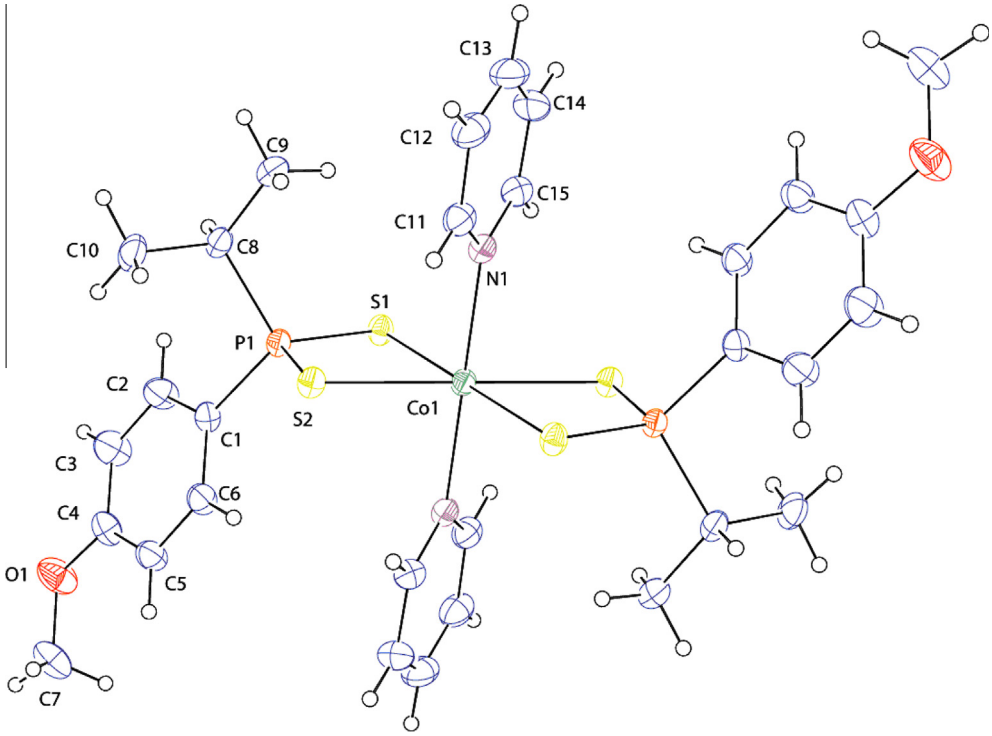

Fig. 6. An ORTEP-3 [40] view of **7** with the atom-numbering scheme. The thermal ellipsoids are drawn at the 50% probability level.

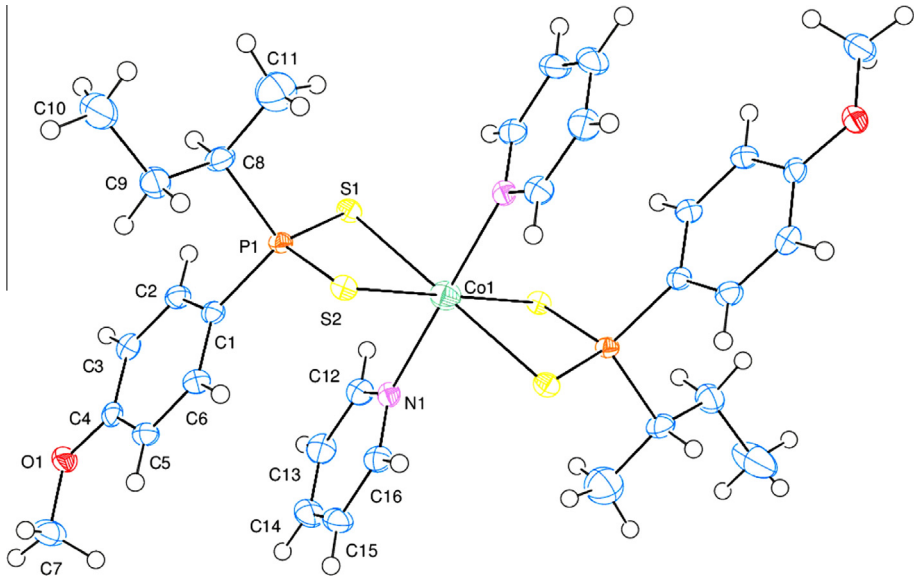

Fig. 7. An ORTEP-3 [40] view of **8** with the atom-numbering scheme. The thermal ellipsoids are drawn at the 50% probability level.

dihedral angle between the two phenyl rings [(C1–C6) and (C11–C16)] is 63.99(5)°, and they are oriented with respect to the pyridine ring (N1/C21–C25) at dihedral angles of 42.41(5)° and 86.92(6)°, respectively. In compounds **7**, **8** and **9**, the Co1 atoms have slightly distorted octahedral coordinations with the symmetry related four-S atoms at the corners of the slightly distorted squares and two symmetry related pyridine N atoms at distances of 2.1731(15) Å, 2.169(3) Å and 2.1825(14) Å, respectively. The dihedral angles between the phenyl and pyridine rings are 61.46(7)°, 12.74(13)° and 28.39(6)°, respectively.

In compounds **5** and **7**, some C–H…π interactions [C7–H7A…Cg2^{i}, where H7A…Cg2^{i} = 2.94 Å, C7…Cg2^{i} = 3.736(2) Å, C7–H7A…Cg2^{i} = 141° and Cg2 is the centroid of the phenyl (C11–C16) ring, symmetry code (i): −1 + *x*, 1 + *y*, *z* (for **5**) and C12–H12…Cg1^{i}, where H12…Cg1^{i} = 2.97 Å, C12…Cg1^{i} = 3.738(3) Å, C12–H12…Cg1^{i} = 141° and Cg1 is the centroid of the phenyl (C1–C6) ring, symmetry code (i): 1 + *x*, *y*, *z* (for **7**)] are observed. In the crystal structures, the molecules are elongated along the *c*-axis and stacked along the *b*-axis for complex **5** (Fig. SM4), while they are elongated along the *b*-axis and stacked along the *a*-axis for complex **7** (Fig. SM5). In the crystal structure of complex 7, two π…π interactions of 3.9793(12) Å and 3.9432(10) Å between the four-membered (Co1/S1/S2/P1) and pyridine (N1/C11–C15) rings [Cg1…Cg3 = 3.9793(12) Å and Cg1…Cg3^{i} = 3.9432(10) Å,

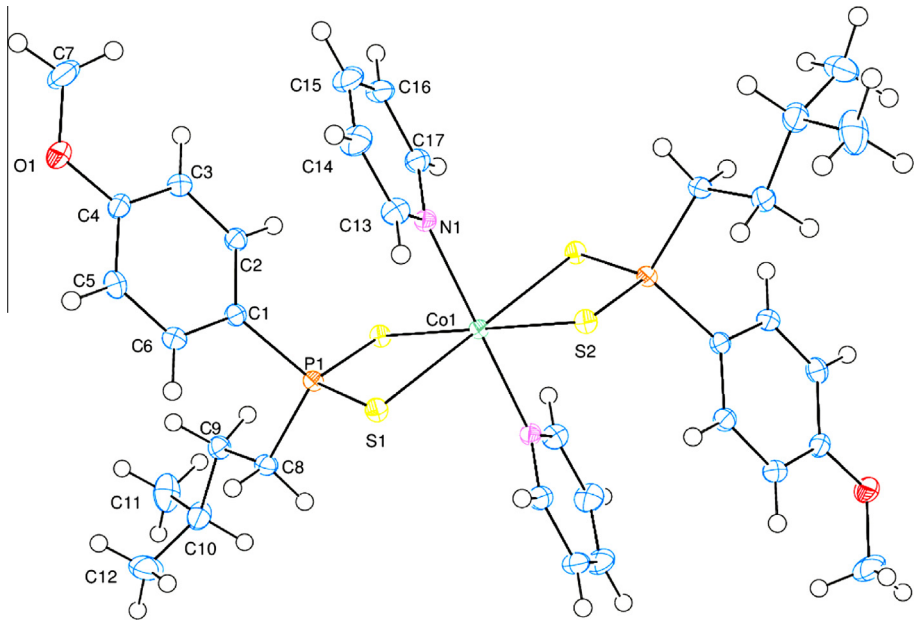

Fig. 8. An ORTEP-3 [40] view of **9** with the atom-numbering scheme. The thermal ellipsoids are drawn at the 50% probability level.

where Cg1 and Cg3 are the centroids of (Co1/S1/S2/P1) and (N1/C11–C15) rings, symmetry code (i): $-x$, $1-y$, $1-z$] are also observed. In the crystal structures of compounds **8** and **9**, intermolecular C–H…O hydrogen bonds [C2–H2…O1^{i}, where H2…O1^{i} = 2.43 Å, C2…O1^{i} = 3.267(5) Å and C2–H2…O1^{i} = 150°, symmetry code (i): $-x+1/2$, $y-½$, $-z-½$ (for **8**) and C6–H6…O1^{i}, where H6…O1^{i} = 2.55 Å, C6…O1^{i} = 3.457(2) Å, C6–H6…O1^{i} = 164°, symmetry code (i): $-x-½$, $y-½$, $-z+½$ (for **9**)] link the molecules into two dimensional networks (Figs. SM6 and SM7). In the crystal structure of compound **8**, a π…π interaction of 3.716(2) Å [Cg1…Cg2 = 3.716(2) Å, where Cg1 and Cg2 are the centroids of phenyl (C1–C6) and pyridine (N1/C12–C16) rings] is also observed.

4. Conclusions

Four-coordinated DTPA complexes of cobalt(II) can bind to one or two molecules of pyridine to form five-and six-coordinated, mixed complexes whereas nickel complexes of the same nature can only form six-coordinated counterparts.

The ^{13}C NMR spectrum of the nickel(II) complex (**1**) displays remarkable differences from that of the corresponding ligand in that the coupling constant between the adjacent P–C atoms is reduced by more than 10 Hz upon complexation.

The single crystal X-ray analyses of the four cobalt-DTPA-pyridino-complexes reveals that the PS_2^- group is essentially of an electron delocalised structure as reflected in the P–S bond lengths.

The thermal analysis show that the metal-DTPA complexes thermally decompose at around 380 °C to yield the corresponding thiophosphite salt and at around 700 °C, metal-sulfide starts to form.

Acknowledgement

We gratefully acknowledge the financial assistance of Technical Research Council of Turkey (grant number TBAG 114Z091 and TBAG 110T016, TUBITAK). Our thanks also go to Anadolu University; The Research Center for Medicine and Medicinal Plants (BIBAM), Eskişehir, for allowing us to use the X-ray facility therein.

Appendix A. Supplementary material

CCDC 1034096 (for **5**), 1034097 (for **7**), 1034098 (for **8**) and 1034095 (for **9**) contains the supplementary crystallographic data for this paper. These data can be obtained free of charge from The Cambridge Crystallographic Data Centre via www.ccdc.cam.ac.uk/data_request/cif. Supplementary data associated with this article can be found, in the online version, at http://dx.doi.org/10.1016/j.ica.2015.05.028.

References

[1] E.C. Hughes, C. Heights, J.D. Bartleson, US 2,590,430 (1952).
[2] C. Plackowski, W.J. Bruckard, A.V. Nguyen, Miner. Eng. 65 (2014) 61.
[3] S. Arrowsmith, M.D. Irving, US 8,709,988, B2 (2014).
[4] E. Froeschmann, US 5,872,085 (1999).
[5] A.V. Artem'ev, S.F. Malysheva, N.K. Gusarova, N.A. Belogorlova, S.V. Fedorov, B.V. Timokhin, V.I. Smirnov, B.A. Trofimov, Chem. Heterocycl. Comp. 48 (2012) 448.
[6] A.C. Bara, C. Silvestru, I. Haiduc, Anticancer Res. 11 (1991) 1651.
[7] J. Chen, S. Wang, C. Xu, X. Wang, X. Feng, Procedia Chem. 7 (2012) 172.
[8] J. Chen, M. Wei, X. Liu, J. Wang, Prog. Nucl. Energy 54 (2012) 46.
[9] S.M. Ghoreishi, K. Ansari, H.S. Ghaziaskar, J. Supercritical Fluids 72 (2012) 288.
[10] M.M. Rauhut, A.H. Currier, V.P. Wystrach, J. Org. Chem. 26 (1961) 5133.
[11] K. Diemert, W. Kuchen, Sulfur Silicon Relat. Elem. 2 (1977) 131.
[12] W. Kuchen, H. Hertel, Angew. Chem., Int. Ed. Engl. 8 (1969) 89.
[13] R.G. Cavell, W. Byers, E.D. Day, P.M. Watkins, Inorg. Chem. 11 (1972) 1598.
[14] R.G. Cavell, E.D. Day, W. Byers, P.M. Watkins, Inorg. Chem. 11 (1972) 1759.
[15] J.A. McCleverty, R.S.Z. Kowalski, N.A. Bailey, R. Mulvaney, D.A. O'Cleirigh, J. Chem. Soc., Dalton Trans. (1983) 627.
[16] I. Haiduc, Coord. Chem. Rev. 158 (1997) 325.
[17] A.A. Pinkerton, F.P. Ahlers, H.F. Greiwing, B. Krebs, Inorg. Chim. Acta 257 (1997) 77.
[18] J.S. Casas, M.S. García-Tasende, A. Sánchez, J. Sordo, E.E. Castellano, J. Zukerman-Schpector, Inorg. Chim. Acta 219 (1994) 115.
[19] C. Byrom, M.A. Malik, P. O'Brien, A.J.P. White, D.J. Williams, Polyhedron 19 (2000) 211.
[20] M. Calligaris, G. Nardin, A. Ripamonti, J. Chem. Soc., A (1970) 714.
[21] K. Helmut, K. Wilhelm, Phosphorus Sulfur Relat. Elem. 14 (1983) 225.
[22] R.Y. Saleh, D.K. Straub, Inorg. Chem. 13 (1974) 1559.
[23] E.D. Day, R.E.D. McClung, Inorg. Chem. 15 (1976) 571.
[24] R.N. Mukherjee, M.S. Venkateshan, M.D. Zingde, J. Inorg. Nucl. Chem 36 (1974) 547.
[25] E.G. Sağlam, Ö. Çelik, S. İde, H. Yılmaz, Anal. Chem. X-ray Struct., Anal. Online 27 (2011) 23.
[26] T.E. Kokina, L.A. Glinskaya, R.F. Klevtsova, S.V. Larionov, J. Struct. Chem. 43 (2002) 312.
[27] T.E. Kokina, L.A. Glinskaya, E.A. Novoselova, R.F. Klevtsova, S.V. Larionov, J. Struct. Chem. 45 (2004) 855.

[28] R.N. Mukherjee, M.S. Venkateshan, M.D. Zingde, J. Inorg. Nucl. Chem. 36 (1974) 1418.
[29] W. Kuchen, R. Philipp, Z. Anorg. Allg. Chem. 443 (1978) 241.
[30] R.N. Mukherjee, S. Shankar, D.L. Mascarenhas, Indian J. Chem. 25A (1986) 838.
[31] K. Diemert, W. Kuchen, Chem. Ber. 104 (1971) 2592.
[32] W. Kuchen, A. Judat, Chem. Ber. 100 (1967) 991.
[33] J. Delventhal, H. Keck, W. Kuchen, Angew. Chem., Int. Ed. 1 (1972) 830.
[34] T.E. Kokina, L.A. Glinskaya, E.A. Novoselova, R.F. Klevtsova, S.V. Larionov, J. Struct. Chem. 46 (2005) 1031.
[35] P. Porta, A. Sgamellotti, N. Vinciguerra, Inorg. Chem. 10 (1971) 541.
[36] E.G. Sağlam, H. Yılmaz, H. Dal, T. Hökelek, Sulfur Silicon Relat. Elem. 187 (2012) 213.
[37] E.G. Sağlam, Ö. Çelik, H. Yılmaz, S. İde, Transition Met. Chem. 35 (2010) 399.
[38] H. Hoffmann, G. Schumacher, Tetrahedron Lett. 31 (1967) 2963.
[39] G.M. Sheldrick, Acta Crystallogr., Sect. A 64 (2008) 12.
[40] L.J. Farrugia, J. Appl. Crystallogr. 30 (1997) 565.
[41] International Table for X-ray Crystallography (Kynoch Press, Birmingham [Present Distributor Kluwer Academic, Dordrecht] 1974), vol. 4.
[42] S. Sundee, L. Hanlan, J. Bernstein, Inorg. Chem. 14 (1975) 2012.
[43] R. Czernuszewicz, E. Maslowsky Jr., K. Nakamoto, Inorg. Chim. Acta 40 (1980) 199.
[44] M. Noji, Y. Kidani, H. Koike, Bull. Chem. Soc. Japan 48 (1975) 245.
[45] M.C. Aragoni, M. Arca, F. Demartin, F.A. Devillanova, C. Graiff, F. Isaia, V. Lippolis, A. Tiripicchio, G. Verani, J. Chem. Soc., Dalton Trans. (2001) 2671.
[46] M. Karakuş, H. Yılmaz, E. Bulak, P. Lonnecke, Appl. Organomet. Chem. 19 (2005) 396.
[47] T.A. Albright, W.J. Freeman, E.E. Schweizer, J. Org. Chem. 40 (1975) 3437.
[48] M. Chakravarty, S. Pailloux, S. Ouizem, K.A. Smith, E.N. Duesler, R.T. Paine, N.J. Williams, R.D. Hancock, Polyhedron 33 (2012) 327.
[49] H. Keck, W. Kuchen, Phosphorus Sulfur Relat. Elem. 14 (1983) 225.
[50] S. Heinz, H. Keck, W. Kuchen, Org. Mass Spoctrom. 19 (1984) 82.
[51] D. Christoph, H. Keck, W. Kuchen, J. Mathow, H. Wunderlich, Inorg. Chim. Acta 132 (1987) 213.
[52] P.N. Mohan, W. Kuchen, H. Keck, G. Haegele, J. Inorg.Nucl. Chem. 39 (1977) 833.
[53] D. Cremer, J.A. Pople, J. Am. Chem. Soc. 97 (1975) 1354.